

# Inarticulate past: Incomplete similarity of the ice-climate system and its implications for paleo-records attribution

Mikhail Y. Verbitsky

Gen5 Group, LLC, Newton, MA, USA  
UCLouvain, Earth and Life Institute, Louvain-la-Neuve, Belgium  
Correspondence: Mikhail Verbitsky (verbitskys@gmail.com)

**Abstract.** Reconstruction and explanation of past climate evolution using proxy records is the essence of paleoclimatology. In this study, we use dimensional analysis of a dynamical model on orbital time-scales to recognize theoretical limits of such forensic inquiries. Specifically, we demonstrate that incomplete similarity does not imply physical similarity and therefore major past events could have been produced by different physical processes making the task of paleo-records attribution to a particular phenomenon to be fundamentally difficult, if not impossible. It also means that any future scenario may not have a unique cause and, in this sense, the orbital time-scale future may be to some extent less sensitive to specific terrestrial circumstances.

## Introduction

Interpretation of most prominent events of climate history such as the middle-Pleistocene transition (Ruddiman et al., 1986, Lisiecki and Raymo, 2005, Clark et al., 2021) has been an inspiration for several generations of climate modelers (see for a review Saltzman, 2002, Clark, et al., 2006, Tziperman et al., 2006, Crucifix, 2013, Mitsui and Aihara, 2014, Paillard, 2015, Ashwin and Ditlevsen, 2015, Verbitsky et al., 2018, Willeit et al., 2019, Riechers et al., 2021). While specific physical mechanisms invoked to explain changing glacial rhythmicity vary, they all include slow changes of ocean-atmosphere governing parameters (e.g., Saltzman and Verbitsky, 1993; Raymo, 1997; Paillard and Parrenin, 2004) or glaciation parameters (Clark and Pollard, 1998). On a more general level, all these theories in fact assume slow changes in the intensities of positive (such as, for example, long-term variations in carbon dioxide concentration, e.g., Saltzman and Verbitsky, 1993) or negative (for example, regolith erosion, Clark and Pollard, 1998, or vertical temperature advection in ice sheets, Verbitsky and Crucifix, 2021) system feedbacks. Though all physical phenomena invoked are, indeed, real and may be plausible, the following question still remains unanswered: Is it possible to disambiguate the past and elevate a single “correct” theory? Answering this question is the goal of our study.

Indeed, this is the classical attribution challenge that has been successfully addressed in the context of another well-known problem of geophysics: the causality of the observed global warming. For this purpose, the most comprehensive space-resolving models have been employed to reproduce observed time-series under different conditions and to prove (or discredit) a candidate physical phenomenon (e.g., Stocker, 2014). Certainly, these models cannot be employed on extremely long orbital time-scales (10 – 100 kyr) due to computational constraints. In search for an alternative, we turn here to dimensional analysis. Historically, dimensional analysis and concepts of similarity have been used for studying physical phenomena, complementing even the most sophisticated computational tools and providing physical insight in situations where physical interpretation of the higher-complexity modeling results may be difficult. Here, on orbital timescales, when we retreat from physics-abundant space-resolving models to more conceptual dynamical models, dimensional analysis may be promoted from a supporting to a more prominent, prophetic, role.

Several key terms need to be introduced before we outline the structure of our paper. We will be using the definitions of physical similarity and complete and incomplete similarity as they have been articulated by G. I. Barenblatt (2003). Suppose we have a physical phenomenon that is governed by  $n$  physical parameters,  $k$  parameters of which are parameters with independent dimensions. Then, according to the  $\pi$ -theorem (Buckingham, 1914), the phenomenon can be described by  $n-k$  adimensional similarity parameters  $\pi_1, \pi_2, \dots, \pi_i, \dots, \pi_{n-k}$ . We will consider two phenomena as being physically similar if they are described by identical similarity parameters  $\pi_1, \pi_2, \dots, \pi_i, \dots, \pi_{n-k}$ . The dimensionless time series of physically similar processes are also identical. If a similarity parameter  $\pi_i$  can be excluded from the description of a physical process (a phenomenon becomes independent of it in the limit that  $\pi_i$  tends to zero or infinity) we can talk about complete similarity of this physical process in this parameter: regardless of its specific value, the process does not depend on it. And, finally, we may have incomplete similarity when none of similarity parameters  $\pi_1, \pi_2, \dots, \pi_i, \dots, \pi_{n-k}$  can be neglected even if they are too small (or too big), but the

53 number of effective parameters may still be reduced because a phenomenon depends not on absolute value of  
 54 similarity parameters but on their products in some power degree (i.e., conglomerate groups):

55  $\Pi_j = (\pi_1^{\alpha_j})(\pi_2^{\beta_j}) \dots (\pi_l^{\lambda_j}) \dots (\pi_{n-k}^{\chi_j})$  ( $j = 1, 2, \dots, l; l < n - k$ ). Here  $\alpha_j, \beta_j, \dots, \lambda_j, \dots, \chi_j$  are power degrees  
 56 of  $\pi_1, \pi_2, \dots, \pi_l, \dots, \pi_{n-k}$  involved into  $\Pi_j$  formulation.

57 We are now ready to proceed with the structure of our paper: (a) first, we will introduce our dynamical  
 58 model and describe major physical processes involved; (b) using dimensional analysis, we will define 8 similarity  
 59 parameters  $\pi_1 - \pi_8$  that completely define model's behavior; (c) while these adimensional similarity  
 60 parameters  $\pi_1 - \pi_8$  will be determined using simple rules of dimensional analysis, there are no specific algorithms  
 61 that can help us in finding their effective conglomerate groups  $\Pi_j$ , if they indeed exist. Therefore, we will articulate  
 62 such conglomerate groups based on observed system behavior; (d) we will then discuss implications of our findings  
 63 for the attribution challenge and illustrate our reasoning with a numerical experiment; (e) we will conclude our study  
 64 with some thoughts relating our results to the real-world climate system.

## 66 Method

67  
 68 For our experiments we employ the Verbitsky et al (2018), VCV18 thereafter, dynamical model of the ice-  
 69 climate system. It has been derived from the scaled mass- and heat-balance equations of the non-Newtonian ice  
 70 flow, i.e., equations (1) and (2), correspondingly, and combined with an energy-balance equation of the global  
 71 climate temperature (3):

$$72 \frac{dS}{dt} = \frac{4}{5} \zeta^{-1} S^{3/4} (a - \varepsilon F_S - \kappa \omega - c \theta) \quad (1)$$

$$73 \frac{d\theta}{dt} = \zeta^{-1} S^{-1/4} (a - \varepsilon F_S - \kappa \omega) \{ \alpha \omega + \beta [S - S_0] - \theta \} \quad (2)$$

$$74 \frac{d\omega}{dt} = -\gamma [S - S_0] - \frac{\omega}{\tau} \quad (3)$$

75  
 76 Here,  $S$  ( $\text{m}^2$ ) is the area of glaciation,  $\theta$  ( $^{\circ}\text{C}$ ) is the basal ice-sheet temperature, and  $\omega$  ( $^{\circ}\text{C}$ ) is the global  
 77 temperature of the ocean-atmosphere (rest of the climate) system. In deriving equations (1) and (2) we considered  
 78 ice sheets in the thin-boundary-layer approximation such that their inertial forces are negligible relative to stress  
 79 gradients, and motion equations with very high accuracy can be written in a quasi-static form. For such  
 80 approximation, a characteristic ice thickness  $H$  is connected to ice area  $S$  as  $H = \zeta S^{1/4}$  where  $\zeta$  ( $\text{m}^{1/2}$ ) is a profile  
 81 factor assumed to be constant (Verbitsky and Chalikov, 1986, VCV18). Further, equation (1) represents global ice  
 82 balance  $\frac{d(HS)}{dt} = AS$ , where, again,  $H = \zeta S^{1/4}$  and  $A = a - \varepsilon F_S - \kappa \omega - c \theta$  is the surface mass influx. Equation (2)  
 83 describes vertical ice temperature advection with a time scale  $H/(a - \varepsilon F_S - \kappa \omega)$ , and equation (3) is the global  
 84 energy-balance equation. The parameter  $a$  ( $\text{m s}^{-1}$ ) is the snow precipitation rate;  $F_S$  is normalized external forcing,  
 85 specifically, mid-July insolation at  $65^{\circ}\text{N}$  (Berger and Loutre, 1991) of the amplitude  $\varepsilon$  ( $\text{m s}^{-1}$ ) such that  $\varepsilon F_S$  describes  
 86 ice ablation rate due to astronomical forcing;  $\kappa \omega$  is the ice ablation rate representing the cumulative effect of the  
 87 global climate on ice-sheet mass balance;  $c \theta$  represents ice discharge due to ice-sheet basal sliding;  $\alpha \omega$  is basal  
 88 temperature response to global climate temperature change,  $\beta [S - S_0]$  is basal temperature reaction to the changes  
 89 of ice geometry;  $-\gamma [S - S_0]$  describes global temperature response to ice geometry changes (e.g., albedo);  $\kappa$  ( $\text{m s}^{-1}$   
 90  $^{\circ}\text{C}^{-1}$ ),  $c$  ( $\text{m s}^{-1} ^{\circ}\text{C}^{-1}$ ),  $\alpha$  (adimensional),  $\beta$  ( $^{\circ}\text{C m}^{-2}$ ) and  $\gamma$  ( $^{\circ}\text{C m}^{-2} \text{s}^{-1}$ ) are sensitivity coefficients;  $S_0$  ( $\text{m}^2$ ) is a reference  
 91 glaciation area; and  $\tau$  (s) is the timescale for  $\omega$ . When orbitally forced, the model reproduced events of the last  
 92 million years reasonably well, except for the interglacial of 400 kyr ago (marine isotopic stage 11). The timing of all  
 93 other interglacials coincides with Past Interglacial Working Group of PAGES (2016) data (VCV18).

94 We will now focus on the most remarkable feature of the historical records - a period  $P$  of climate response  
 95 to the astronomical forcing. Indeed, it is the change of the climate variability from the predominant period  $P = 40$   
 96 kyr to the main periods of  $P = 80$ -120 kyr that makes the middle-Pleistocene transition so extraordinary. Though the  
 97 amplitude increase was considered, until recently, to be a necessary attribute of this transition, its presence in the  
 98 paleo-records is now questioned (Clark et al, 2021). We begin with the dimensional analysis of the VCV18 system  
 99 (1) – (3). Indeed, it has 11 governing parameters (including the amplitude  $\varepsilon$  and the period  $T$  of the external forcing).  
 100 If we choose  $\varepsilon$ ,  $T$  and  $\gamma$  to be parameters with independent dimensions, then in accordance with  $\pi$ -theorem a period  
 101 of the system response can be fully described by 8 dimensionless similarity parameters  $\pi_1 - \pi_8$ :

102

103  $\pi_1 = \frac{\varepsilon}{a}, \pi_2 = \alpha, \pi_3 = \kappa\gamma\varepsilon T^3, \pi_4 = c\gamma\varepsilon T^3, \pi_5 = \frac{T}{\tau}, \pi_6 = \frac{\gamma T}{\beta}, \pi_7 = \frac{S_0}{\varepsilon^2 T^2}, \pi_8 = \frac{\zeta}{\varepsilon^{1/2} T^{1/2}},$  and

104  
105 
$$P = T\Psi(\pi_1, \pi_2, \dots, \pi_8) \tag{4}$$

106  
107 At the same time, we observed earlier (Verbitsky and Crucifix, 2020) that the period of the system (1) – (3) response  
108 to the obliquity forcing of period  $T$  is mostly governed by two dimensionless parameters: by the ratio of the  
109 astronomical forcing amplitude to terrestrial ice sheet snow precipitation rate,  $\varepsilon/a$ , and by the adimensional  $V$ -  
110 number. The physical meaning of the  $V$ -number in the orbital domain becomes most evident if we take a closer look  
111 into the structure of positive and negative feedbacks as they appear in the system (1) – (3). The time-dependent  
112 negative feedback is proportional to the ice sheet area size as  $\beta(S - S_0)$ . The coefficient  $\beta$  is defined by  
113 thermodynamical properties of an ice sheet, most importantly by the Peclet number,  $Pe = \hat{A}H/k$ ,  $\hat{A}$  is a  
114 characteristic mass influx, i.e., accumulation minus ablation and  $k$  is ice temperature diffusivity (VCV18, Verbitsky  
115 and Crucifix, 2021). This negative feedback acts on ice-sheet mass balance with a vertical-advection time delay and  
116 is amplified by a sensitivity coefficient  $c$  that reflects the intensity of basal sliding. The time-dependent positive  
117 feedback is global temperature  $\omega$ . In the orbital domain,  $\tau \ll T$  ( $\pi_5 \gg 1$ ),  $\omega$  is approximately proportional  
118 to  $-\gamma\tau(S - S_0)$ . The global temperature acts on the ice-sheet mass balance “instantly” as  $\kappa\omega$  and with the vertical-  
119 advection time-delay as a component of basal temperature conditions,  $\alpha\omega c$ . Thus, the  $V$ -number is emerging in the  
120 orbital domain as a ratio of amplitudes of time-dependent positive and negative feedbacks.

121  
122 
$$V = \frac{\gamma\tau}{\beta c}(\alpha c + \kappa) \tag{5}$$

123  
124 Specifically, when  $V \sim 0.75$  and  $\varepsilon/a \sim 1$ , the system exhibits the obliquity-period doubling. When the positive  
125 feedback and the obliquity forcing are less articulated, the system responds with the 40-kyr period. Thus, slow  
126 changes of the  $V$ -number (for example, from  $V = 0.5$  at  $t = 3,000$  kyr ago to  $V = 0.75$  at  $t = 0$ ) and of the  $\varepsilon/a$  ratio (for  
127 example, from  $\varepsilon/a = 0.3$  to  $\varepsilon/a = 1.7$  over the same time span) produce a change in the ice-climate behavior similar  
128 to the middle-Pleistocene transition.

129 We now notice that the  $V$ -number can be presented in terms of similarity parameters  $\pi_1 - \pi_8$ , specifically:

130  
131 
$$V = \frac{\gamma\tau}{\beta c}(\alpha c + \kappa) = \left(\pi_2 + \frac{\pi_3}{\pi_4}\right) \frac{\pi_6}{\pi_5} \tag{6}$$

132  
133 We also experimentally established that the period-doubling sustains ( $\Psi = 2$ ) if, under fixed  $\varepsilon/a$  and  $V$ , the period  
134 of the external forcing changes from let say  $T = 35$  kyr to  $T = 50$  kyr. It can only happen if in this domain similarity  
135 parameters  $\pi_7$  and  $\pi_8$  make another conglomerate group that does not depend on  $T$ , specifically  $\frac{\pi_8^4}{\pi_7}$ .

136 Thus, equation (4) can be written as:

137  
138 
$$P = T\Psi\left(\pi_1, \frac{\pi_2\pi_6}{\pi_5}, \frac{\pi_3\pi_6}{\pi_4\pi_5}, \frac{\pi_8^4}{\pi_7}\right), \tag{7}$$

139  
140 that is the pure case of incomplete similarity as we defined it above. Finally we may notice that  $\frac{\pi_8^4}{\pi_7} = \frac{H^4}{S_0^2} \ll 1$  for all  
141 large ice sheets (thin-boundary-layer approximation). If we set it to be constant and apply generalized  $\pi$ -theorem  
142 (Sonin, 2004) we can re-write equation (7) in a more simple form as

143  
144 
$$P = T\Psi\left(\frac{\varepsilon}{a}, V\right) \tag{8}$$

145  
146 Recognition of incomplete similarity is important because it provides us with a powerful insight: different  
147 combinations of similarity parameters  $\pi_i$  may produce the same  $V$ -number, i.e., *physically unsimilar processes*  
148 (formed by not identical  $\pi_i$ ) *may cause the same outcome*. This observation is critical for our attribution challenge.  
149 Certainly, precise disambiguation of historical records is always a difficult task because even two physically similar  
150 processes having identical adimensional similarity parameters and demonstrating the same behavior may have been  
151 produced by different values of physical parameters involved, unless these parameters are physical constants or well  
152 defined. The situation becomes especially challenging when we deal with incomplete similarity because, as we just

153 stated, the same results may be produced by not-identical similarity parameters (physically unsimilar processes).  
154 This is the theoretical limit that we aspire to expose.

155 We will now apply our findings to the middle-Pleistocene transition. Since the physical interpretation of the  
156 governing parameters incorporated in the conglomerate  $V$ -number is very straightforward, we may observe a similar  
157 (in terms of the period- $P$  bifurcation) system response to changes of a completely different physical nature. For  
158 example, parameter  $\beta$ , as we have discussed above, defines intensity of the negative feedback and is formed as a  
159 result of interplay between vertical ice advection, internal friction, and geothermal heat flux (VCV18). Increased  
160 Peclet number of the growing ice sheet diminishes the role of the geothermal heat flux and may reduce parameter  $\beta$   
161 thus increasing the  $V$ -number. The same period- $P$  bifurcation can also be caused, for example, by slow changes in  
162 the parameter  $\gamma$  that defines the intensity of the positive feedback and incorporates effects of the albedo change or  
163 other atmospheric feedbacks. We solve equations (1) – (3) for two cases we have just described. In both cases we  
164 invoke a global cooling trend. In our first experiment (Fig. 1a), this trend is translated into reduction of  $\beta$ , i.e.,  
165 weakening of the ice sheet negative feedback, and corresponding increase of the  $V$ -number from  $V = 0.5$  to  $V = 0.75$ .  
166 We assume here that in growing ice sheets the role of the geothermal heat flux is diminished. The increased  
167 continentality of the climate (reduced intensity of the snowfall during colder climate) is accounted by the  $\varepsilon/a$  ratio  
168 increase from  $\varepsilon/a = 0.3$  to  $\varepsilon/a = 1.7$ . In the second experiment (Fig. 1b), the  $V$ -number also evolves from  $V = 0.5$  to  $V$   
169  $= 0.75$ , but this time it is achieved by increased intensity of the positive feedback ( $\gamma$ ). The millennial forcing is added  
170 to  $\varepsilon F_{\zeta}$  as a single sinusoid of 5 kyr period and doubled ( $2\varepsilon$ ) amplitude. In both experiments, we used mid-July  
171 insolation at 65°N (Berger and Loutre, 1991) for the last 3 million years as an astronomical forcing. It is important  
172 to note that in the first experiment (changing  $a$  and  $\beta$ ) only similarity parameters  $\pi_1$  and  $\pi_6$  are being changed, but in  
173 the second experiment (changing  $a$  and  $\gamma$ ) the same changes of the  $V$ -number are caused by changing  $\pi_1, \pi_3, \pi_4, \pi_6$ .  
174 It means that the processes involved in these two experiments are not physically similar. Though the time-series  
175 produced in these two cases are obviously non-identical (see Fig. 1 inserts), we can observe that different physical  
176 phenomena may produce the same changes in the conglomerate  $V$ -number and the same large-scale effect, i.e., the  
177 period-doubling bifurcation at about 1 Myr ago.

178 We do not attempt here to fully reproduce paleo-records such as the Lisiecki and Raymo (2005) or Clark et al.  
179 (2021), and a discussion of whether a period doubling should be accompanied by the amplitude increase is outside  
180 of the current paper's scope. We will just remark that the amplitude of the system response is the function of not just  
181 the period  $P$  but also of the  $\varepsilon/a$  ratio (Verbitsky and Crucifix, 2020) and, for example, less articulated continentality  
182 of colder climates may explain diminished amplitude contrasts as it has been recently advocated by Clark et al  
183 (2021).

184 Indeed, as we have already indicated, we used mid-July insolation at 65°N (Berger and Loutre, 1991) for the  
185 last 3 million years as an astronomical forcing. Apart from that, these examples may also serve as an illustration of  
186 some future scenarios of the climate system behavior under post-industrial atmospheric carbon dioxide  
187 concentration reduction as implied by Ridgwell and Hargreaves (2007). Again, regardless of the physical nature of  
188 the underlying dynamical system, it exhibits 40-kyr rhythmicity of the first 1.5 million years of its evolution and  
189 consequent obliquity-period doubling. This probable renaissance of ice-ages is different from the one envisioned by  
190 Talento and Ganapolski (2021) which is based on the model tuned to the late Pleistocene (last 800 kyr) ice-volume  
191 data and thus postulates only 100-kyr-period variability for the future.

## 192 Conclusions

194 The idea of the current presentation is simple but its implication may be important: If ice-climate system has a  
195 property of incomplete similarity, then we may be limited in our ability to disambiguate historical records and  
196 different physical processes may produce same future scenarios. The latter is intriguing because since B. Saltzman  
197 (1962) and E. Lorenz (1963) had discovered a hydrodynamic system's sensitivity to initial conditions, the concept of  
198 deterministic chaos became a dominant concept of weather and climate theory. Our findings suggest that if we  
199 consider orbital time scales and, instead of time series, focus on their more generalized attributes such as the period  
200 of the system response to the astronomical forcing, we may observe that the behavior of these attributes may be, to  
201 some extent, less sensitive to the physical nature of the terrestrial governing processes.

202 But is incomplete similarity of the global, orbital-scale, climate system real? So far, this property has been  
203 found only in our VCV18 low-order dynamical model, and although this model has been explicitly derived from the  
204 conservation laws, the incomplete similarity of the ice-climate system will remain hypothetical until it is supported  
205 by empirical data. We speculate, though, that existing historical records may provide some support to this concept.  
206 To evaluate the feasibility of a diagnostic approach, let us entertain a simple scaling exercise. Suppose that an  
207 empirical time series, such as  $\delta^{18}\text{O}$  record, is created by a parent system (other than the VCV18) which is controlled

208 by  $n$  physical parameters ( $k$  of them having independent dimensions). If we choose the period of the astronomical  
209 forcing  $T$  to be among parameters with independent dimensions, then in accordance with the  $\pi$ -theorem we have:

$$210 \quad P = T\Psi(\pi_1, \pi_2, \dots, \pi_{n-k}) \quad (9)$$

211  
212  
213 The wavelet spectrum of the late Pleistocene  $\delta^{18}\text{O}$  variability in response to the precession ( $\sim 20$ -kyr period) and  
214 obliquity ( $\sim 40$ -kyr period) forcing shows the dominance of 40-kyr and 80-kyr periods (Fig. 1c). If we are willing to  
215 accept it as a hint of  $\Psi = 2$  for  $T = 20$  kyr and for  $T = 40$  kyr, then, since some of the similarity parameters  
216  $\pi_1, \pi_2, \dots, \pi_{n-k}$  depend on  $T$ , the period- $T$  independence of  $\Psi$  may only happen when  $\pi_1, \pi_2, \dots, \pi_{n-k}$  make  
217 conglomerate  $T$ -independent groups. In other words, *period independence of the  $\Psi$  function may be a signature of*  
218 *climate system incomplete similarity*. Indeed, the diagnostics of the  $\Psi$  function may require much more sophisticated  
219 instruments than our *ad hoc* reasoning, and the records will likely not explicitly reveal what the conglomerate  
220 similarity groups look like; nevertheless, their mere existence would corroborate the idea of this paper.

221 **Competing interests:** The author declares that he has no conflict of interest.

222 **Acknowledgements:** The author is grateful to Michel Crucifix for multiple discussions related to this topic **and to**  
223 **two anonymous reviewers for their helpful comments.**

## 224 **References**

225  
226  
227 Ashwin, P. and Ditlevsen, P.: The middle Pleistocene transition as a generic bifurcation on a slow manifold, *Clim.*  
228 *Dynam.*, 45, 2683–2695, <https://doi.org/10.1007/s00382-015-2501-9>, 2015.

229  
230 Barenblatt, G. I.: *Scaling*, Cambridge University Press, Cambridge, 2003.

231  
232 Berger, A. and Loutre, M. F.: Insolation values for the climate of the last 10 million years, *Quaternary Sci. Rev.*, 10,  
233 297–317, 1991.

234  
235 Buckingham, E.: On physically similar systems; illustrations of the use of dimensional equations, *Phys. Rev.*, 4,  
236 345–376, 1914.

237  
238 Clark, P. U. and Pollard, D.: Origin of the middle Pleistocene transition by ice sheet erosion of regolith,  
239 *Paleoceanography*, 13, 1–9, 1998.

240  
241 Clark, P. U., Archer, D., Pollard, D., Blum, J. D., Rial, J. A., Brovkin, V., Mix, A. C., Pisias, N. G., and Roy, M.:  
242 The middle Pleistocene transition: characteristics, mechanisms, and implications for long-term changes in  
243 atmospheric  $\text{pCO}_2$ , *Quaternary Sci. Rev.*, 25, 3150–3184, 2006.

244  
245 Clark, P. U., Shakun, J., Rosenthal, Y., Köhler, P., Schrag, D., Pollard, D., Liu, Z., and Bartlein, P.: Requiem for the  
246 Regolith Hypothesis: Sea-Level and Temperature Reconstructions Provide a New Template for the Middle  
247 Pleistocene Transition. No. EGU21-13981. Copernicus Meetings, 2021.

248  
249 Crucifix, M.: Why could ice ages be unpredictable?, *Clim. Past*, 9, 2253–2267, [https://doi.org/10.5194/cp-9-2253-](https://doi.org/10.5194/cp-9-2253-2013)  
250 2013, 2013.

251  
252 Lisiecki, L. E. and Raymo, M. E.: A Pliocene-Pleistocene stack of 57 globally distributed benthic  $\delta^{18}\text{O}$  records,  
253 *Paleoceanography*, 20, PA1003, <https://doi.org/10.1029/2004PA001071>, 2005.

254  
255 Lorenz, E.N.: Deterministic nonperiodic flow, *Journal of atmospheric sciences*, 20, 2, 130-141, 1963.

256  
257 Mitsui, T. and Aihara, K.: Dynamics between order and chaos in conceptual models of glacial cycles, *Clim. Dynam.*,  
258 42, 3087–3099, 2014.

259  
260 Paillard, D.: Quaternary glaciations: from observations to theories, *Quaternary Sci. Rev.*, 107, 11–24,  
261 <https://doi.org/10.1016/j.quascirev.2014.10.002>, 2015.

262

263 Paillard, D. and Parrenin, F.: The Antarctic ice sheet and the triggering of deglaciations, *Earth Planet. Sc. Lett.*, 227,  
264 263–271, 2004.

265

266 **Past Interglacial Working Group of PAGES: Interglacials of the last 800,000 years, *Rev. Geophys.*, 54, 162–219,**  
267 **2016.**

268

269 Raymo, M.: The timing of major climate terminations, *Paleoceanography*, 12, 577–585,  
270 <https://doi.org/10.1029/97PA01169>, 1997.

271

272 Ridgwell, A., and Hargreaves, J. C.: Regulation of atmospheric CO<sub>2</sub> by deep-sea sediments in an Earth system  
273 model. *Global Biogeochemical Cycles* 21, no. 2, <https://doi.org/10.1029/2006GB002764>, 2007.

274

275 **Riechers, K., Mitsui, T., Boers, N., and Ghil, M.: Orbital Insolation Variations, Intrinsic Climate Variability, and**  
276 **Quaternary Glaciations, *Clim. Past Discuss.* [preprint], <https://doi.org/10.5194/cp-2021-136>, in review, 2021.**

277

278 Ruddiman, W. F., Raymo, M., and McIntyre, A.: Matuyama 41,000-year cycles: North Atlantic Ocean and northern  
279 hemisphere ice sheets, *Earth Planet, Sc, Lett.*, 80, 117–129, [https://doi.org/10.1016/0012-821X\(86\)90024-5](https://doi.org/10.1016/0012-821X(86)90024-5), 1986.

280

281 Saltzman, B.: Finite amplitude free convection as an initial value problem—I, *Journal of atmospheric sciences*, 19,  
282 4, 329-341, 1962.

283

284 Saltzman, B.: Dynamical paleoclimatology: generalized theory of global climate change, in: Vol. 80, Academic  
285 Press, San Diego, CA, 2002.

286

287 Saltzman, B. and Verbitsky, M. Y.: Multiple instabilities and modes of glacial rhythmicity in the Plio-Pleistocene: a  
288 general theory of late Cenozoic climatic change, *Clim. Dynam.*, 9, 1–15, 1993.

289

290 **Sonin, A. A.: A generalization of the  $\Pi$ -theorem and dimensional analysis, *P. Natl. Acad. Sci. USA*, 101, 8525–**  
291 **8526, 2004.**

292

293 Stocker, T. (Ed.): *Climate change 2013: the physical science basis: Working Group I contribution to the Fifth*  
294 *assessment report of the Intergovernmental Panel on Climate Change*, Cambridge University Press, Chapter 10:  
295 *Detection and Attribution of Climate Change: from Global to Regional*, 867–952, 2014.

296

297 **Talento, S. and Ganopolski, A.: Reduced-complexity model for the impact of anthropogenic CO<sub>2</sub> emissions on**  
298 **future glacial cycles, *Earth Syst. Dynam.*, 12, 1275–1293, <https://doi.org/10.5194/esd-12-1275-2021>, 2021.**

299

300 Tziperman, E., Raymo, M. E., Huybers, P., and Wunsch, C.: Consequences of pacing the Pleistocene 100 kyr ice  
301 ages by nonlinear phase locking to Milankovitch forcing, *Paleoceanography*, 21, PA4206,  
302 <https://doi.org/10.1029/2005PA001241>, 2006.

303

304 **Verbitsky, M. Y. and Chalikov, D. V.: *Modelling of the Glaciers-Ocean-Atmosphere System*, Gidrometeoizdat,**  
305 **Leningrad, 1986.**

306

307 Verbitsky, M. Y. and Crucifix, M.:  $\pi$ -theorem generalization of the ice-age theory, *Earth Syst. Dynam.*, 11, 281–  
308 289, <https://doi.org/10.5194/esd-11-281-2020>, 2020.

309

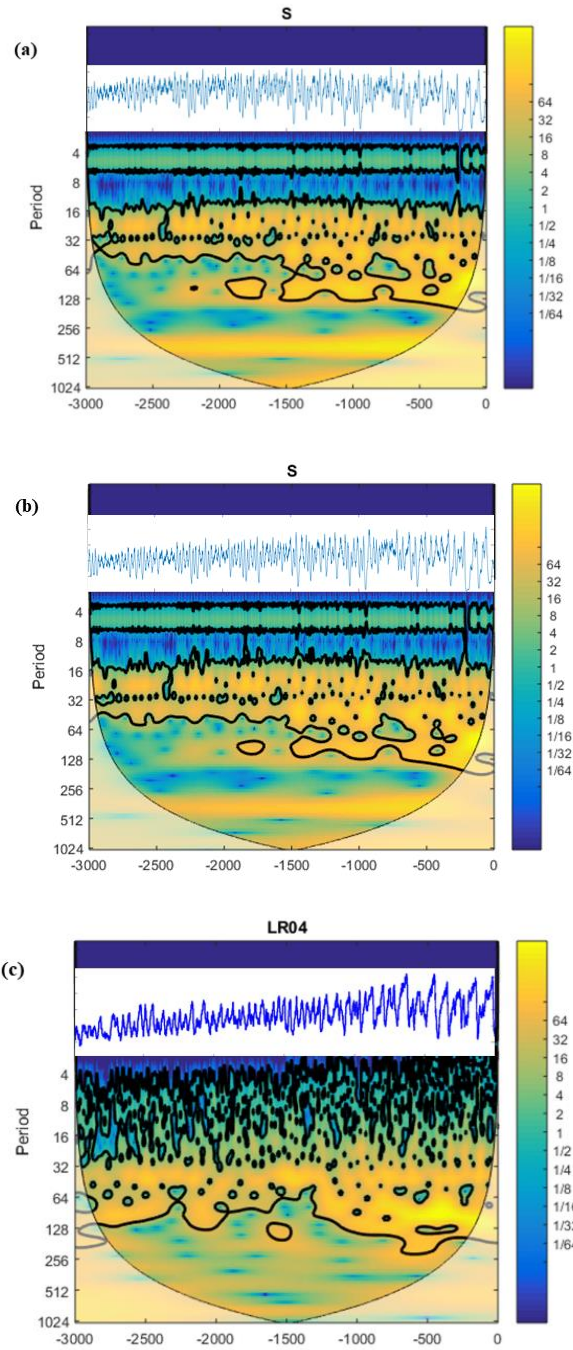
310 **Verbitsky, M. Y. and Crucifix, M.: ESD Ideas: The Peclet number is a cornerstone of the orbital and millennial**  
311 **Pleistocene variability, *Earth Syst. Dynam.*, 12, 63–67, <https://doi.org/10.5194/esd-12-63-2021>, 2021.**

312

313 Verbitsky, M. Y., Crucifix, M., and Volobuev, D. M.: A theory of Pleistocene glacial rhythmicity, *Earth Syst.*  
314 *Dynam.*, 9, 1025–1043, <https://doi.org/10.5194/esd-9-1025-2018>, 2018.

315

316 **Willeit, M., Ganopolski, A., Calov, A., and Brovkin, V.: Mid-Pleistocene transition in glacial cycles explained by**  
317 **declining CO<sub>2</sub> and regolith removal, *Science Advances* 5, 4, <https://www.science.org/doi/10.1126/sciadv.aav7337>,**  
318 **2019**



319 **Fig. 1** Ice-climate system response to a cooling trend presented as an evolution of wavelet spectra over 3 Myr for  
 320 calculated ice-sheet glaciation area  $S$  ( $10^6 \text{ km}^2$ ) – panels (a) and (b), and for the Lisiecki and Raymo (2005) benthic  
 321  $\delta^{18}\text{O}$  record, panel (c). The  $V$ -number evolves from  $V = 0.5$  to  $V = 0.75$  due to weakening of the negative feedback  
 322 (a) and due to intensified positive feedback (b). **The vertical axis is the period (kyr), the horizontal axis is time (kyr**  
 323 **before present).** The color scale shows the continuous Morlet wavelet amplitude, the thick line indicates the peaks  
 324 with 95 % confidence, and the shaded area indicates the cone of influence for wavelet transform. **Inserts are**  
 325 **corresponding time series.**